J|A|C|S
ARTICLES
Published on Web 09/13/2006

The Si−Si Effect on Ionization of β-Disilanyl Sulfides and Selenides

Richard S. Glass,*,† Eric Block,‡ Edward Lorance,§ Uzma I. Zakai,† Nadine E. Gruhn,† Jin Jin,‡ and Shao-Zhong Zhang‡

Contribution from the Departments of Chemistry, The University of Arizona, Tucson, Arizona 85721, University at Albany, State University of New York, Albany, New York 12222, and Vanguard University, Costa Mesa, California 92626

Received October 27, 2005; Revised Manuscript Received July 7, 2006; E-mail: rglass@u.arizona.edu

Abstract: The ionization energies of conformationally constrained, newly synthesized β-disilanyl sulfides and selenides were determined by photoelectron spectroscopy. These ionization energies reflect substantial (0.53−0.75 eV) orbital destabilizations. The basis for these destabilizations was investigated by theoretical calculations, which reveal geometry-dependent interaction between sulfur or selenium lone pair orbitals and σ-orbitals, especially Si−Si σ-orbitals. These results presage facile redox chemistry for these compounds and significantly extend the concept of σ-stabilization of electron-deficient centers.

Introduction

Silyl,[1] germyl,[2] and stannyl[2] groups are well-known to strongly stabilize β-carbocations (M−C−C$^+$) and weakly stabilize β-carbon-centered radicals (M−C−C$^\bullet$).[3] This β-effect is believed to result mainly from hyperconjugative resonance by the M−C σ-bond, which requires favorable orbital overlap of the M−C σ-bond and the empty carbocation p-orbital or half-occupied carbon radical p-orbital. The requirement for orbital overlap is well-illustrated by the kinetic acceleration in solvolysis of geometrically constrained β-silyl sulfonates, which is dependent upon the torsional angle between the Si−C σ-bond and the C−O σ-bond attaching the leaving group. That is, for β-silyl sulfonates, the better the overlap of the Si−C σ-bond with the developing p-orbital of the incipient carbocation, the faster the rate of solvolysis. In a similar way, $SiCH_2$ moieties are also powerful activators and ortho/para-directors in electrophilic aromatic substitution. It has also been reported that β-Si−Si σ-bonds stabilize benzyl[4] and cyclopropyl[5] cations of general structure Si−Si−C$^+$. This β-effect is ascribed to Si−Si σ-bond hyperconjugation, dramatically illustrated by the lack of such stabilization when the β-Si−Si σ-bond is orthogonal to the leaving group.[4a] Even more remote γ- and δ-effects of silicon and tin on carbocations have been reported.[6] The β-effect of silicon and tin has also been evaluated at heteroatom radical cation centers (M−C−E$^{+\bullet}$) in place of carbocations or carbon-centered radicals. Thus the electrochemical oxidation potentials of β-silyl ethers and amines are significantly lower than those of the corresponding nonsilylated ethers and amines.[7] In addition, although the effect of β-silyl groups on the oxidation potential of sulfides and selenides is more modest than with ethers and amines,[7b,d] the effect of β-stannyl groups is substantial.[7h,8,9] Stabilization by the β-effect of the radical cations obtained on oxidation is believed to account for these results. Mixing of the SOMO and Si−C orbitals in the radical cations

† The University of Arizona.
‡ University at Albany.
§ Vanguard University.

(1) (a) Bassindale, A. R.; Taylor, P. G. In *The Chemistry of Organic Silicon Compounds*; Patai, S., Rappoport, Z., Eds.; Wiley: Chichester, 1989; Part 2, pp 893−963. (b) Siehl, H.-U.; Müller, T. In *The Chemistry of Organic Silicon Compounds*; Rappoport, Z., Apeloig, Y., Eds.; Wiley: Chichester, 1989; Vol. 2, pp 595−701. (c) Lambert, J. B. *Tetrahedron* **1990**, *46*, 2677−2689. (d) Lambert, J. B.; Liu, X. *J. Organomet. Chem.* **1996**, *521*, 203−210. (e) Lambert, J. B.; Zhao, Y.; Emblidge, R. W.; Salvador, L. A.; Liu, X.; So, J.-H.; Chelius, E. C. *Acc. Chem. Res.* **1999**, *32*, 183−190. (f) Brook, M. A. *Silicon in Organic, Organometallic and Polymer Chemistry*; Wiley: New York, 2000. (g) Müller, T.; Margraf, D.; Syha, Y. *J. Am. Chem. Soc.* **2005**, *127*, 10852−10860.

(2) (a) Lambert, J. B.; Wang, G.; Teramura, D. H. *J. Org. Chem.* **1988**, *53*, 5422−5428. (b) Nguyen, K. A.; Gordon, M. S.; Wang, G.; Lambert, J. B. *Organometallics* **1991**, *10*, 2798−2803.

(3) (a) Landais, Y. *C.R. Chimie* **2005**, *8*, 823−832. (b) Kawamura, T.; Kochi, J. K. *J. Am. Chem. Soc.* **1972**, *94*, 648−650.

(4) (a) Shimizu, N.; Kinoshita, C.; Osajima, E.; Hayakawa, F.; Tsuno, Y. *Bull. Chem. Soc. Jpn.* **1991**, *64*, 3280−3288. (b) Shimizu, N.; Watanabe, S.; Hayakawa, F.; Yasuhara, S.; Tsuno, Y.; Inazu, T. *Bull. Chem. Soc. Jpn.* **1994**, *67*, 500−504.

(5) Shimizu, N.; Hayakawa, F.; Tsuno, Y. *Bull. Chem. Soc. Jpn.* **1992**, *65*, 959−964.

(6) (a) Lambert, J. B.; Salvador, L. A.; So, J.-H. *Organometallics* **1993**, *12*, 697−703. (b) Sugawara, M.; Yoshida, J. *J. Am. Chem. Soc.* **1997**, *119*, 11986−11987. (c) Sugawara, M.; Yoshida, J. *J. Org. Chem.* **2000**, *65*, 3135−3142.

(7) (a) Cooper, B. E.; Owen, W. J. *J. Organomet. Chem.* **1971**, *29*, 33−40. (b) Block, E.; Yencha, A. J.; Aslam, M.; Eswarakrishnan, V.; Luo, J.; Sano, A. *J. Am. Chem. Soc.* **1988**, *110*, 4748−4753. (c) Bock, H.; Meuret, J.; Stein, U. *J. Organomet. Chem.* **1990**, *398*, 65−77. (d) Bock, H.; Meuret, J. *J. Organomet. Chem.* **1993**, *459*, 43−54. (e) Yoshida, J.; Maekawa, T.; Murata, T.; Matsunaga, S.; Isoe, S. *J. Am. Chem. Soc.* **1990**, *112*, 1962−1970. (f) Yoshida, J. *Top. Curr. Chem.* **1994**, *170*, 39−81. (g) Yoshida, J.; Tsujishima, H.; Nakuno, K.; Isoe, S. *Inorg. Chim. Acta* **1994**, *220*, 129−135. (h) Yoshida, J.; Nishiwaki, K. *J. Chem. Soc., Dalton Trans.* **1998**, 2589−2596.

(8) (a) Glass, R. S.; Radspinner, A. M.; Singh, W. P. *J. Am. Chem. Soc.* **1992**, *114*, 4921−4923. (b) Glass, R. S.; Guo, Q.; Liu, Y. *Tetrahedron* **1997**, *53*, 12273−12286. (c) Li, H.; Nishiwaki, K.; Itami, K.; Yoshida, J. *Bull. Chem. Soc. Jpn.* **2001**, *74*, 1717−1725.

(9) The reason for the greater effectiveness of a C−Sn σ-MO than C−Si σ-MO is a better energy match of orbital energies and consequent greater interaction. That is, the HOMO ionization energy for sulfur 3p lone pair orbitals in thioethers is much lower than that of oxygen and nitrogen lone pair orbitals in ethers and amines. Consequently, while a C−Si σ-MO is a good energy match for an oxygen or nitrogen lone pair orbital, the lower energy C−Sn σ-MO is a better energy match for a sulfur or selenium lone pair HOMO than a C−Si σ-MO.

derived from silyl-substituted ethers and sulfides has been shown by EPR spectroscopy.[10]

To address the stabilization of sulfur and selenium radical cations by a γ-(Si−Si) bond (Si−Si−C−$E^{+\bullet}$, E = S, Se), a series of new cyclic β-disilanyl sulfides and selenides were synthesized and studied. These conformationally constrained compounds were investigated because preliminary theoretical calculations indicated that interaction of a sulfide or selenide p-orbital with a γ-(Si−Si) σ-MO should be geometry dependent. This paper reports application of photoelectron spectroscopy as a tool for revealing these γ-(Si−Si) effects.[11]

Experimental Results on Conformationally Constrained Heterocycles

Photoelectron Spectroscopy. Photoelectron spectroscopy (PES) is the experimental technique used in this study to evaluate γ-(Si−Si)[19] stabilization of sulfur and selenium radical cations.[16,20] Although this technique explicitly measures the energy difference between radical cations and corresponding neutral states, the measured vertical ionization energies for valence shell electrons are generally discussed in terms of Koopmans' theorem. That is, the ionization energy equals the negative of the orbital eigenvalue (or energy), and the photoelectron spectra reported here then are interpreted in terms of molecular orbital energies of the un-ionized neutral compound and not the corresponding radical cations. Nevertheless, this approach is useful for determining the stabilization by Si−Si bonds of chalcogen radical cations for two reasons. First, the orbital interactions of substituents on a filled chalcogen p-type orbital are analogous to those in the half-filled p-orbital of the radical cation. Second, PES ionization energies generally correlate with electrochemical oxidation potentials of organochalcogen compounds.[16,22]

Table 1. Fit Parameters for PES (all energies in eV)

			Relative Area	
Gaussian	position	half-width high, low	He I	He II/He I
2a				
1	7.98	0.57, 0.57	1.00	
2	8.43	0.52, 0.52	0.87	
3	9.17	0.84, 0.84	1.45	
2b				
1	7.89	0.31, 0.29	1.00	
2	8.32	0.57, 0.57	0.83	
3	8.76	0.56, 0.56	0.76	
5a				
1	7.62	0.39, 0.39	1.00	1.00
2	8.00	0.37, 0.37	1.01	0.93
3	8.58	0.61, 0.61	0.81	1.81
4	8.89	0.61, 0.61	0.84	2.85
5b				
1	7.45	0.33, 0.33	1.00	1.00
2	7.80	0.35, 0.35	1.19	1.16
3	8.56	0.63, 0.63	0.74	2.09
4	8.82	0.60, 0.60	0.74	1.69
7a				
1	7.87	0.47, 0.30	1.00	
2	8.87	0.71, 0.69	0.64	
8a				
1	7.51	0.34, 0.34	1.00	
2	7.73	0.32, 0.32	0.83	
3	8.09	0.39, 0.39	0.89	
4	8.37	0.38, 0.38	0.82	
5	8.83	0.47, 0.47	0.89	
11a				
1	7.80	0.35, 0.34	1.00	
2	8.17	0.42, 0.39	0.90	
3	9.49	0.58, 0.58	1.16	
4	9.47	0.48, 0.39	1.00	

A variety of previously unknown organo−sulfur and −selenium compounds were synthesized[23] and studied by gas-phase PES and theoretical calculations. Due to the cyclic nature of these compounds, they are geometrically constrained to different conformations. Two parameters that can be used to define the geometry about the moieties of interest, illustrated in **1**, are the dihedral angle about the RS−CSi bond, θ, and the dihedral angle about the SC−SiSi bond, ϕ.[24]

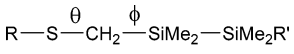

1

In the following section, the experimental results on the compounds studied are organized based on these dihedral angles, which were deemed especially relevant because of the known geometry dependence of Si−C and chalcogen lone pair orbital interactions and the anticipated geometry dependence of Si−Si and chalcogen lone pair orbital interactions. The ionization energies reported are based on deconvolutions of the data with asymmetric Gaussians (see Experimental Section); complete fitting parameters for all compounds discussed are listed in Table 1.

***θ* ca. 0°, *ϕ* ca. 120°.** Compounds **2a** and **2b** were chosen for study because they might be expected to adopt nearly planar ring geometries where the C−Si σ-orbital and sulfur/selenium p-orbitals do not interact as shown in **3** (which also is the case

(10) Kira, M.; Nakazawa, H.; Sakurai, H. *Chem. Lett.* **1986**, 497−500.
(11) It was anticipated that a Si−Si σ-bond would be more effective than a C−Si σ-bond in stabilizing chalcogen radical cations because of a better energy match. That is, the ionization energy of a Si−Si σ-MO (8.68,[12] 8.69[13] eV for $Me_3Si-SiMe_3$) is lower than that of C−Si σ-MO (10.5 eV)[14] and a better energy match for a sulfur or selenium HOMO (the ionization energy for dialkyl sulfides is 8.1−8.7 eV).[15−17] Lowering of the ionization energy by a β-Si−Si σ-MO has been reported[18] for 2,2-bis(trimethylsilyl)-1,3-dithia-2-silacyclopent-4-ene.
(12) Mochida, K.; Itani, A.; Yokoyama, M.; Tsuchiya, T.; Worley, S. D.; Kochi, J. K. *Bull. Chem. Soc. Jpn.* **1985**, *58*, 2149−2150.
(13) Bock, H.; Ensslin, W. *Angew. Chem., Int. Ed. Engl.* **1971**, *10*, 404−405.
(14) Bock, H.; Solouki, B. In *The Chemistry of Organic Silicon Compounds*; Patai, S., Rappoport, Z., Eds.; Wiley: Chichester, UK, 1989; Part 1, pp 555−563.
(15) (a) Bock, H.; Wagner, G. *Angew. Chem., Int. Ed. Engl.* **1972**, *111*, 150−151. (b) Wagner, G.; Bock, H. *Chem. Ber.* **1974**, *107*, 68−77. (c) Gleiter, R.; Spanget-Larsen, J. *Top. Curr. Chem.* **1979**, *86*, 140−195.
(16) Glass, R. S.; Wilson, G. S.; Coleman, B. R.; Setzer, W. N.; Prabhu, U. D. G. *Adv. Chem. Ser.* **1982**, *201*, 417−441.
(17) Trofimov, B. A.; Mel'dev, U. Kh.; Pikver, R. I.; Vyalykh, E. P. *Theor. Exp. Chem. (Engl.)* **1975**, *11*, 129−135.
(18) Tsutsui, S.; Takahashi, M.; Sakamoto, K. *Chem. Lett.* **2000**, 1376−1377.
(19) Bock, H.; Solouki, B. *Chem. Rev.* **1995**, *95*, 1161−1190.
(20) For use of photoelectron spectroscopy to probe the interaction of Si−Si σ-MOs with adjacent π-systems in tetrasila[2.2]paracyclophane, see: Gleiter, R.; Schäfer, W.; Krennrich, G.; Sakurai, H. *J. Am. Chem. Soc.* **1988**, *110*, 4117−4120.
(21) Since the time scale for PES ionization is much shorter than that for electrochemical oxidation, the correlation breaks down when there is significant molecular reorganization on removal of an electron. See ref 22 for examples.
(22) (a) Glass, R. S.; Andruski, S. W.; Broeker, J. L.; Firouzabadi, H.; Steffen, L. K.; Wilson, G. S. *J. Am. Chem. Soc.* **1989**, *111*, 4036−4045. (b) Block, E.; Birringer, M.; DeOrazio, R.; Fabian, J.; Glass, R. S.; Guo, C.; He, C.; Lorance, E.; Qian, Q.; Schroeder, T. B.; Shan, Z.; Thiruvazhi, M.; Wilson, G. S.; Zhang, X. *J. Am. Chem. Soc.* **2000**, *122*, 5052−5064.
(23) Block, E.; Dikarev, E. V.; Glass, R. S.; Jin, J.; Li, B.; Li, X.; Zhang, S.-Z. *J. Am. Chem. Soc.*, accepted for publication.

(24) $\theta = 0°$ is defined as shown in **3**; that is, Me and Si are eclipsed. For $\phi = 0°$, S and $SiMe_3$ are eclipsed. The Newman projections shown in **3** and **4** are viewed down the CH_2-S bond with the 3p lone pair orbital on the back sulfur atom drawn.

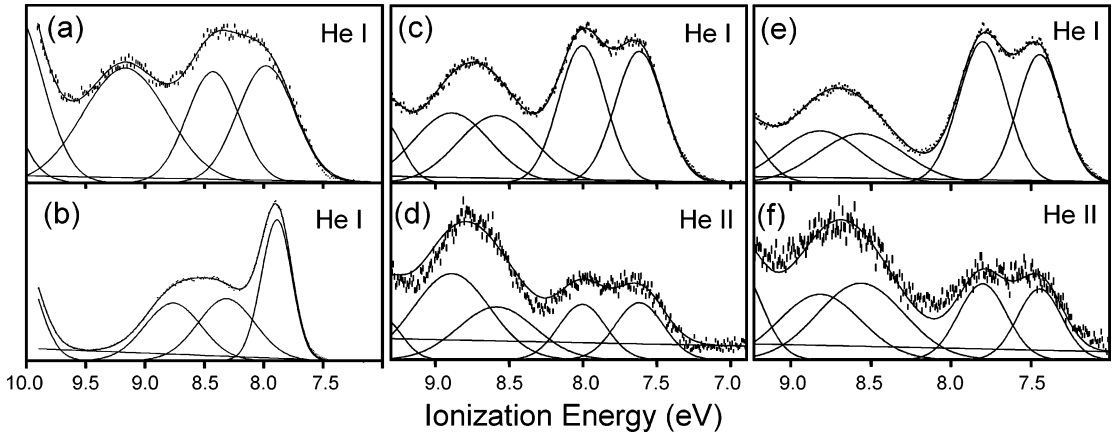

Figure 1. PES (He I or He II, as noted) of (a) **2a**, (b) **2b**, (c, d) **5a**, and (e, f) **5b**.

for **4** where $\theta = 180°$), but their ϕ values would optimize Si−Si σ-orbital mixing with the sulfur/selenium p-orbital. Therefore, these compounds would provide a test of the geometry dependence on ϕ of the remote Si−Si σ-orbital interaction with the sulfur p-orbital.

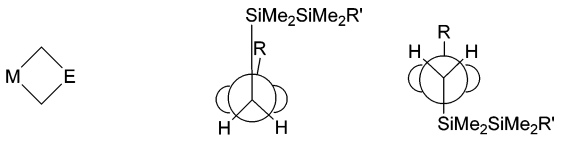

2a, E = S, M = $Si(SiMe_3)_2$
b, E = Se, M = $Si(SiMe_3)_2$
c, E = S, M = CH_2
d, E = S, M = $SiMe_2$

3, θ = 0°

4, θ = 180°

In the solid state, the four-membered rings in both 3,3-bis(trimethylsilyl)-1,3-thiasiletane (**2a**)[25] and the selenium analogue 3,3-bis(trimethylsilyl)-1,3-selenasiletane (**2b**) are planar as determined by X-ray crystallography.[23] Furthermore, computations show that in the gas phase the four-membered ring of compound **2a** is close to planar in its lowest energy conformation with $\theta = 11°$ and $\phi = 100, 126°$.

The PES of **2a** is shown in Figure 1a. The two lowest energy ionization bands in this spectrum are difficult to deconvolute because they are very close in energy and the bands overlap. Assignment of the ionization bands of **2a** is facilitated by analysis of the PES of **2b**, shown in Figure 1b. The geometry of **2b**, $\theta = 8.5°$ and $\phi = 99, 127°$, is very similar to that of **2a** so that orbital interactions should be analogous. However, owing to the lower ionization energy of a selenium 4p lone pair compared to that of a sulfur 3p lone pair, the lowest ionization band of **2b** moves to lower energy and the ionization envelope is also sharper, resulting in much reduced overlap of the lowest energy ionization with the next ionization band.

The amount of destabilization caused by the presence of the Si−Si bond in **2a** can be judged by comparing the lowest vertical ionization (HOMO) energies[26] for thietane (**2c**) (8.55[16,28] and 8.65[17] eV), 3,3-dimethyl-1,3-thiasiletane (**2d**) (8.49 eV[29]), and **2a** (7.98 eV). There is only a modest destabilization of the HOMO (0.06 eV) upon introducing a 3-Me_2Si moiety (i.e., **2d**) but substantial destabilization (0.57 eV) on introducing a 3-$(Me_3Si)_2Si$ moiety (i.e., **2a**) into a thietane ring.

***θ* ca. 180°, *ϕ* ca. 90°.** Compound **5a**, 3,3,4,4,8,8,9,9-octamethyl-1,6-dithia-3,4,8,9-tetrasilecane, adopts a chair, chair, chair conformation in the solid state as shown by X-ray crystallography,[23] and calculations indicate that this conformation is also the most stable in the gas phase. For this conformation, $\theta = 159.6, 156.1°$ and $\phi = 82.1, 78.8°$. The X-ray crystal structure for **5b** is similar to that of **5a**.

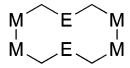

5a, E = S, M = $SiMe_2$
b, E = Se, M = $SiMe_2$
c, E = S, M = CH_2

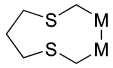

6a, M = $SiMe_2$
b, M = CH_2

These θ values mean that the geometry about the S−C bond is close to that shown in **4**. As depicted in **3** and **4**, the sulfur lone pair and C−Si orbital interactions are the same for $\theta = 180°$ as for $\theta = 0°$. Consequently, orbital interactions for **5a** with $\theta =$ ca. 180° and $\phi =$ ca. 90° should be comparable to those for **2a**.[30] However, since there are two interacting chalcogen atoms in this system, there is an additional factor important in its analysis. That is, there will be symmetric and antisymmetric orbitals combining both sulfur 3p lone pair orbitals. In mesocyclic dithioethers,[31,32] the antisymmetric lone pair combination is the HOMO and the symmetric combination HOMO-1.

The He I and He II PE spectra of **5a** are shown in Figure 1c and 1d, respectively; the He I and He II PE spectra of the selenium analogue **5b** were also measured and are shown in Figure 1e and 1f, respectively. The PE spectra of **5a** and **5b** are

(25) The four-membered ring in 3,3-dimethyl-2,2,4,4-tetraphenyl-1,3-thiasiletane is also planar: Strohmann, C. *Chem. Ber*. **1995**, *128*, 167−172.
(26) Correlation of lowest energy vertical ionization energies determined by PES and ionization potentials determined by charge transfer spectroscopy with tetracyanoethylene (TCNE) in CH_2Cl_2 as the electron acceptor has been reported.[15b,16,27] In general, a linear correlation between the two measurements for the compounds reported in this paper has been found (manuscript in preparation).
(27) Frey, J. E.; Aiello, T.; Beaman, D. N.; Hutson, H.; Lang, S. R.; Puckett, J. J. *J. Org. Chem*. **1995**, *60*, 2891−2901.
(28) Mollere, P. D.; Houk, K. N. *J. Am. Chem. Soc*. **1977**, *99*, 3226−3233.
(29) Traven, V. F.; Rokitskaya, V. T.; Rodin, O. G.; Shvets, V. F.; Redchenko, V. V.; Voronkov, M. G.; Kirpichenko, S. V.; Suslova, E. N. *Dokl. Akad. Nauk SSSR* **1986**, *288*, 1160−1163.
(30) Nevertheless, direct comparison between **2a** and **5a** must be viewed with caution because of other differences in orbital interactions. For example, in **2a**, the two Si−Si σ-orbitals in the Si−Si−Si moiety combine to form π-like orbitals.
(31) Setzer, W. N.; Coleman, B. R.; Wilson, G. S.; Glass, R. S. *Tetrahedron* **1981**, *37*, 2743−2747.
(32) Setzer, W. N.; Glass, R. S. In *Conformational Analysis of Medium-Sized Sulfur-Containing Heterocycles*; Glass, R. S., Ed.; VCH: Weinheim, Germany, 1988; pp 151−179.

also very similar, with the lowest energy region of the spectra shown in Figure 1c and 1d best modeled with four Gaussians; however, the two Gaussians at lowest ionization energy are better separated from the third in the spectrum of **5b** than in that of **5a**. Upon comparing the He I and He II PES of **5b**, the two lowest ionization bands decrease in relative area compared to the third on going from He I to He II. Since the photoionization cross-section for selenium-based orbitals decreases 16-fold more than that for silicon-based orbitals,[33] the two lowest ionizations at 7.45 and 7.80 eV must be from predominantly selenium-based orbitals, whereas that at 8.56 eV is from a predominantly silicon-based orbital. Similarly, the two lowest energy ionizations for **5a** are ascribed to predominantly sulfur-based orbitals and the third and fourth at higher ionization energy to predominantly silicon-based orbitals. Comparison of the sulfur lone pair ionization energies for **5a** (7.62 and 8.00 eV) with those of 1,6-dithiecane **5c** (8.38 and 8.53 eV[16,31]) reveals substantial destabilization in **5a** relative to **5c**. The destabilization of the ionization from HOMO-1 of **5a** relative to **5c** (0.53 eV) is comparable to the destabilization of the ionization from the HOMO of **2a** relative to **2c** (0.57 eV). Destabilization of the first and second ionization energies is also found for **6a**, 7,7,8,8-tetramethyl-1,5,7,8-dithiadisilolane, compared with **6b**, but this system was not analyzed in detail.[34]

***θ* = 0°, *ϕ* = 30°.** While the crystal structure of 3,3,4,4-tetramethyl-1,3,4-thiadisilolane (**7a**) could not be determined, the lowest energy structure found computationally is an envelope conformation in which the sulfur atom is out of the plane of the ring C−Si−Si−C atoms; that is, there is a C−S−C flap.

7a, E = S, M = $SiMe_2$
b, E = S, M = CH_2

This conformation is found to be 2 kcal/mol more stable than any other conformation. In this conformation, the C−S−C−Si (θ) and S−C−Si−S (ϕ) dihedral angles are 50 and 30°, respectively, which indicates that the C−Si σ-orbital, the Si−Si σ-orbital, and sulfur lone pair orbital can interact.

The PES of **7a** (Figure 2a) shows ionizations of lowest energy at 7.87 and 8.87 eV. These ionizations are assigned to the sulfur 3p lone pair and Si−Si σ-bond ionizations, respectively, based on analogy. The HOMO ionization energy for this compound is 0.57 eV lower than that for thiolane, **7b** (7.87 versus 8.44,[16] 8.64 eV[17]).

***θ* = 60−120°, *ϕ* ca. 180°.** Calculations on 3,3,7,7-tetrakis-(trimethylsilyl)-1,5-dithia-3,7-disilocane (**8a**) show that conformer **9** (twist−twist with a C_2 axis through the ring Si atoms) is the most favorable in the gas phase, but conformer **10**, which is found in the solid state by X-ray crystallography,[23] is only 0.4 kcal/mol higher in energy. The calculated dihedral angles for **9** and **10** are approximately $\theta = 119°$, $\phi = 163, 74°$ and $\theta = 51, 62°$, $\phi = 177, 57°$, respectively.

(33) Yeh, J. J.; Lindau, I. *Atomic Data and Nuclear Data Tables*, 1985; Vol. 32, No. 1, Jan.

(34) Destabilization of the ionizations from HOMO and HOMO-1 were also found for **6a** (7.86, 8.20 eV) compared with 1,5-dithionane **6b** (8.36, 8.46 eV).[16,31] The PES and fitting parameters of **6a** are given in the Supporting Information. The ionization at 8.82 eV also seen in its PES is silicon-based as shown by intensity changes on going from He I to He II ionization sources.

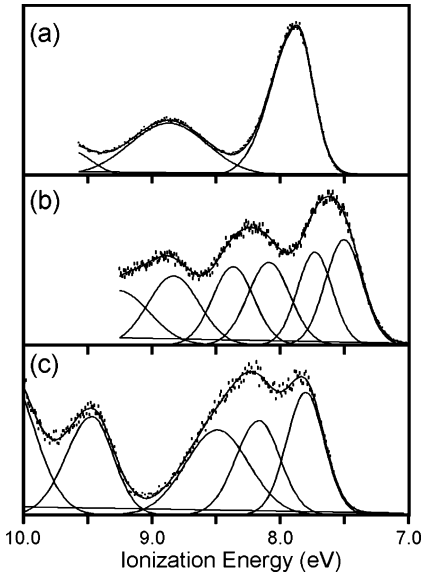

Figure 2. He I PES of (a) **7a**, (b) **8a**, and (c) **11a**.

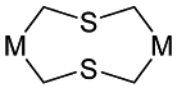

8a, M = $Si(SiMe_3)_2$
b, M = $SiMe_2$
c, M = CH_2

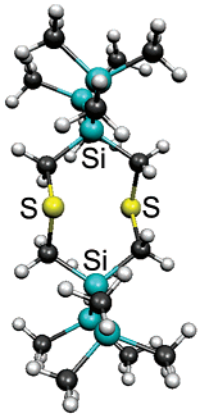

9

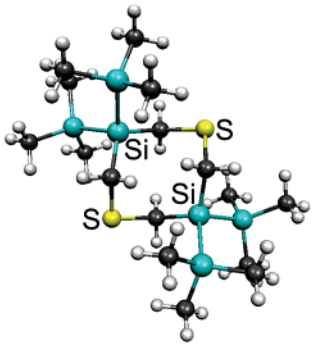

10

The PES for **8a** is shown in Figure 2b. The HOMO ionization energy for **8a** is 0.39 eV lower than that for **8b**, which lacks the Si−Si orbitals but is calculated to have a similar ring geometry as **8a**.[23] In addition, the HOMO ionization for **8a** is 0.70 eV lower than that for 1,5-dithiocane (**8c**).[16,31] This is the largest destabilization observed in this study. The ionization energy for 5,5-bis(trimethylsilyl)-1,3,5-dithiasilinane (**11a**), whose PES is shown in Figure 2c, is also substantially (0.64−0.75 eV) lower than that of 1,3-dithiane (**11b**) (e.g., 7.80 vs 8.55, 8.44[8a] eV).

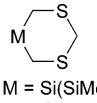

11a, M = $Si(SiMe_3)_2$
b, M = CH_2

Summary of Experimental Results. The photoelectron spectra that have been measured by us show that there is a

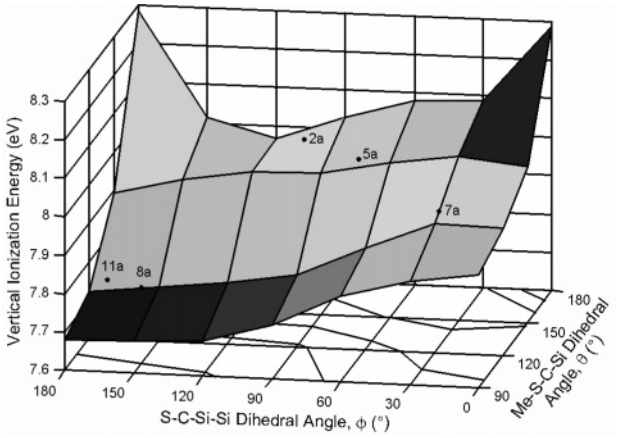

Figure 3. Three-dimensional plot of the vertical ionization energy (eV) for **1**, R = R′ = Me, as a function of θ (Me−S−C−Si dihedral angle, °) and ϕ (S−C−Si−Si dihedral angle, °). Positions of compounds studied experimentally are shown, with the position for compounds with multiple θ or ϕ shown as the one that would maximize interaction.

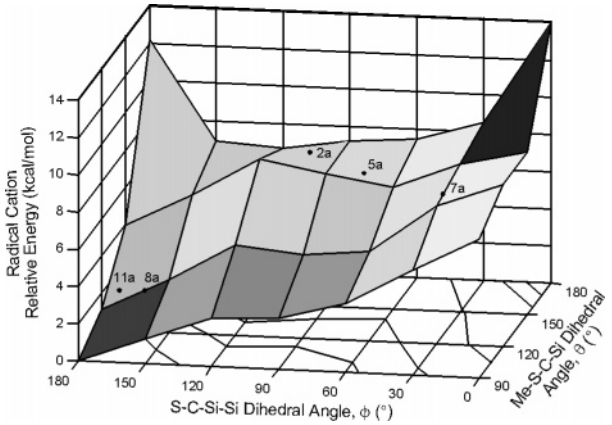

Figure 4. Three-dimensional plot of the relative energy (kcal/mol) of the radical cation of **1**, R = R′ = Me, as a function of θ (Me−S−C−Si dihedral angle, °) and ϕ (S−C−Si−Si dihedral angle, °). Positions of compounds studied experimentally are shown, with the position for compounds with multiple θ or ϕ shown as the one that would maximize interaction.

general destabilization of the chalcogen-based ionizations of these mesocyclic molecules, and that the amount of destabilization observed, which can be as large as 0.70−0.75 eV, is dependent upon the geometry of the mesocycles. To provide insight into the specific orbital interactions that are responsible for these destabilizations as well as providing a more general understanding of σ-lone pair orbital interactions, molecular orbital calculations were carried out as described in the following section.

Theoretical Studies on Model System

To provide a general understanding of the geometry dependence of the sulfur lone pair, Si−Si σ-orbital interactions, theoretical calculations were performed on model compound **1**, R = R′ = Me. This model system allows us to fully explore the geometry influence of changing the dihedral angle about the MeS−CSi bond, θ, and that about the SC−SiSi bond, ϕ,[24] and then apply the results with the model system to the geometrically constrained mesocycles that were studied experimentally. The dihedral angles θ and ϕ were varied, and the corresponding vertical ionization energies and relative energies of the corresponding radical cations were calculated. Three-dimensional plots of these results are shown in Figures 3 and 4, and selected values of vertical ionization energies are given in Table 2. The results show a marked dependence of the ionization energy on geometry. The complete basis for these results are complex, as will be apparent by the detailed theoretical treatment of the conformationally constrained compounds discussed below. Nevertheless, consideration of a few trends and their basis is warranted. With θ fixed at 180°, as shown in **4**, and similarly for $\theta = 0°$ as shown in **3**, the C−Si σ-orbital and the sulfur p-orbital illustrated in the drawings are orthogonal and, therefore, do not interact. If ϕ is now varied, the ionization energy is greatest (most stable HOMO energy) at 0 and 180° and lowest at 120°, with a range of about 0.3 eV.

The reason for a minimum ionization energy at $\phi = 120°$ is that the HOMO is actually comprised of a combination of the sulfur 3p-orbital and the π-like antisymmetric combination of the CH_2 σ-orbitals of the α-CH_2 group. When $\phi = 120°$, the Si−Si and C−H σ-orbitals are eclipsed as depicted in **12** (view down (MeS)CH_2−Si(Me)($SiMe_3$) bond), and there is maximal

Table 2. Calculated Vertical Ionization[a] for **1**, R = R′ = Me, as a Function of Geometry

	θ, °			
ϕ, °	180	150	120	90
0	8.288	8.007	7.932	7.891
30	8.088	8.027	7.936	7.867
60	8.081	8.002	7.864	7.821
90	8.030	7.969	7.788	7.739
120	7.966	7.962	7.760	7.691
150	8.016	7.937	7.740	7.683
180	8.283	7.892	7.721	7.678

[a] Vertical ionization energies listed in the table are in eV.

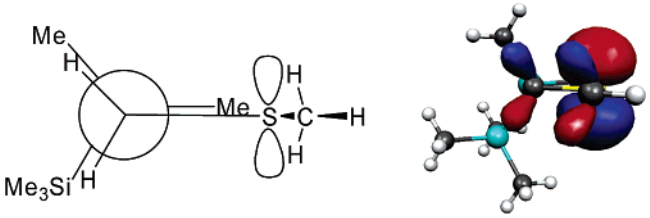

12, θ = 180°, ϕ = 120°

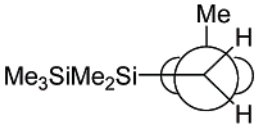

13, θ = 90°

destabilization of the HOMO by the Si−Si σ-orbital. With θ fixed at 90° (see **13**), overlap between the C−Si σ-bond and sulfur p-orbital is maximized. This geometry with $\theta = 90°$ then permits C−Si σ-orbital as well as Si−Si σ-orbital mixing with the sulfur p-orbital. Varying ϕ with $\theta = 90°$ results in a continuous decrease in ionization energy from a maximum at 0° to a minimum at 180° with a change of about 0.2 eV. Comparison of the calculated ionization energy where $\theta = 90°$ with that where $\theta = 180°$ for any value of ϕ shows a decrease of 0.2 eV or greater. Especially notable is the 0.6 eV decrease in calculated ionization energy for $\theta = 90°$ compared to $\theta = 180°$ when $\phi = 180°$. With $\theta = 90°$, $\phi = 180°$, the geometry is optimized for antisymmetric combination of the sulfur 3p-

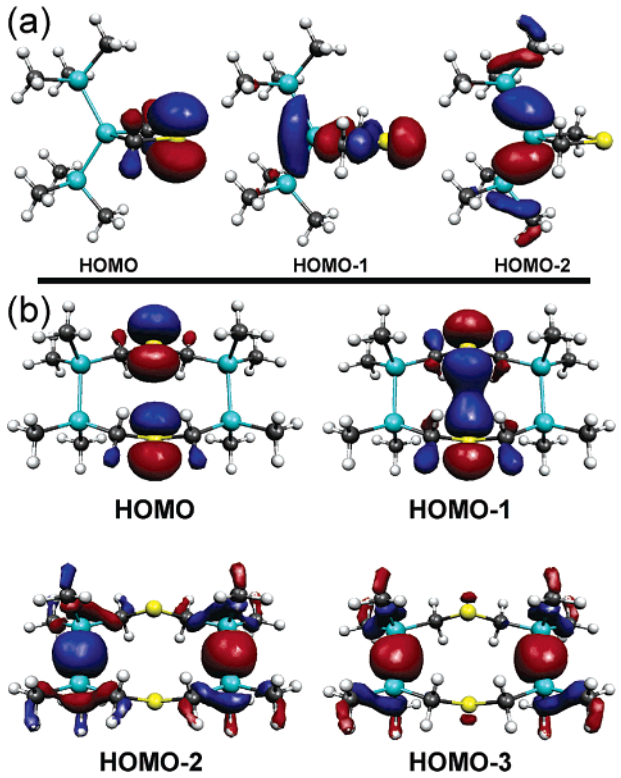

Figure 5. Molecular orbital plots for (a) **2a**, ±0.05 and (b) **5a**, ±0.04.

orbital, C−Si, and Si−Si σ-orbitals as shown in **14** (view with S−C−Si−Si in plane of the paper). With $\theta = 90°$, $\phi = 0°$, **15**, the sulfur 3p-orbital and C−Si σ-orbital but not the Si−Si σ-orbital interact. The Si−Si σ-orbital does not interact in this orientation because the Si atom of the $SiMe_3$ group is in the nodal plane of the antisymmetric sulfur 3p-orbital. Consequently, the net overlap of the Si−Si σ-orbital with the sulfur 3p-orbital is 0.

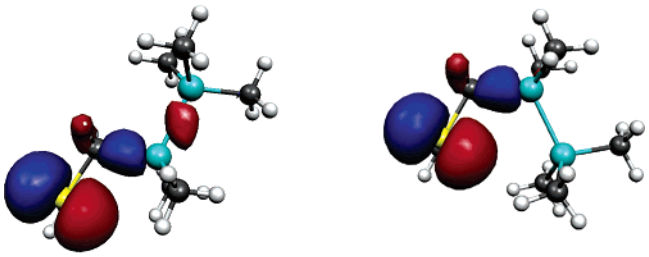

14, θ = 90°, ϕ = 180°

15, θ = 90°, ϕ = 0°

Theoretical Results on Conformationally Constrained Heterocycles

***θ* ca. 0°, *ϕ* ca. 120°.** On the basis of the model calculations, the HOMO for **2a** and, by implication, for **2b**, should be destabilized by π-like CH_2 and Si−Si σ-orbitals. Theoretical calculations were carried out on **2a** and **2b**, and orbital plots for the three MOs of highest energy of **2a** are shown in Figure 5a. The HOMO for **2a** features sulfur 3p lone pair character, but with substantial π-like contribution of the antisymmetric combination of C−H σ-orbitals of the ring CH_2 groups. Such mixing of the sulfur lone pair orbital of b_1 symmetry and ring π-like CH_2 MOs was previously reported[28] for the HOMO of **2c**. This destabilization of the HOMO by the π-like CH_2 σ-orbitals in **2a** and **2b** is analogous to that of **2c** and **2d**, but what accounts for the additional ca. 0.5 eV destabilization of the HOMO of **2a** relative to that of **2c** and **2d**? On the basis of the model system calculations, this could be due to Si−Si σ-orbital interaction. Indeed, computational support for this interaction was obtained by fragment analysis, which was performed by breaking **2a**−**d** into two fragments, one containing only the S or Se atom, respectively, and one containing the rest of the atoms in these molecules. Plots of the sulfur- or selenium-free fragment orbitals that contribute to the HOMO of **2a**−**d**, their percent contributions to the HOMO of **2a**−**d**, and their contribution to the orbital energy of the HOMO of **2a**−**d** are given in the Supporting Information.

The key result is that antisymmetric combinations of the Si−Si σ-orbitals of the $(Me_3Si)_2Si$ group contribute to the HOMO of **2a**. Although the percent contribution of these orbitals to the HOMO of **2a** is modest, they are nonetheless important in terms of their energy contribution to the HOMO of **2a**. That is, the substantial destabilization of the HOMO of **2a** relative to that of **2c** is primarily due to destabilization by these predominantly Si−Si orbitals. Of course, such destabilization is not possible for **2d**, which is devoid of Si−Si orbitals. Consequently, the HOMO and ionization energy of **2d** is only modestly destabilized relative to the HOMO and ionization energy of thietane **2c**.

The HOMO-1 and HOMO-2 of **2a** are also shown in Figure 5a. These orbitals, which are computed to be close in energy in accord with experiment, are highly delocalized. HOMO-1 is composed of Si−Si, C−Si, and C−S σ-orbital and *in-plane* sulfur lone pair character. Mixing of the in-plane sulfur lone pair orbital of a_1 symmetry with the ring C−Si bonds in **2d** has been reported previously.[29,35] HOMO-2 is composed principally of the π-like antisymmetric combination of Si−Si σ-orbitals of the $(Me_3Si)_2Si$ moiety. MO calculations and fragment analysis on the selenium analogue of **2a** (i.e., **2b**) show qualitatively similar results except that there is much more modest mixing in **2b** compared to **2a** owing to the larger difference in energy between Si−Si orbitals and Se 4p lone pair orbitals. Orbital plots of the HOMO, HOMO-1, and HOMO-2 for **2b** are given in the Supporting Information.

***θ* ca. 180°, *ϕ* ca. 90°.** Orbital plots for the HOMO, HOMO-1, HOMO-2, and HOMO-3 for **5a** are shown in Figure 5b. The HOMO in **5a** is the antisymmetric lone pair orbital, which is very similar to the HOMO in **5c**. Fragment analysis results are shown in the Supporting Information. This analysis reveals that the novel π-like antisymmetric combination of an α-C−H and ring C−Si σ-orbital is the major source of the destabilization. The geometry of **5a** appears especially well-suited for this interaction. Here, the HOMO is the antisymmetric 3p sulfur lone pair orbital which is symmetry forbidden from interacting with the Si−Si σ-orbitals. In contrast, the HOMO-1 is the symmetric 3p sulfur lone pair orbital, and mixing between this orbital and the symmetric combination of Si−Si σ-MOs is symmetry allowed, and fragment analysis reveals its importance. This interaction is reminiscent of the mixing of the sulfur 3p lone pair orbitals and C−C σ-MO in 1,4-dithiane (**16**),[36−38] except that for **16** the symmetric HOMO is destabilized while for **5a** it is the symmetric HOMO-1 that is destabilized. The

(35) Rodin, O. G.; Traven, V. F.; Suslova, E. N.; Voronkov, M. G. *J. Mol. Struct.* **1992**, *262*, 1−5.

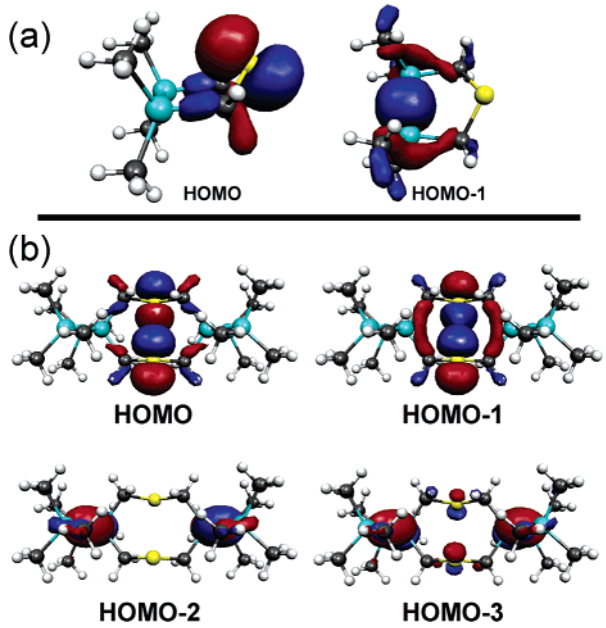

Figure 6. Molecular orbital plots (a) **7a**, ±0.05 and (b) **9**, ±0.04.

destabilization of the ionization from HOMO-1 of **5a** relative to that of **5c** (0.53 eV) is comparable to the destabilization of the ionization from the HOMO of **2a** relative to that of **2c** (0.57 eV).

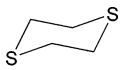

16

***θ* = 0°, *ϕ* = 30°.** Orbital plots of the HOMO and HOMO-1 of **7a** are shown in Figure 6a. As can be seen in this figure, the HOMO for **7a** is predominately sulfur 3p lone pair, but there is mixing of the π-like MOs obtained by combining C−H and C−Si σ-MOs as discussed previously in the analysis of **5a**. This mixing accounts for the destabilization of this HOMO relative to that in thiolane (**7b**). The HOMO-1 of **7a** is predominately Si−Si σ-orbital character with C−Si contributions.

Further insight into the destabilization of the HOMO of **7a** was obtained by fragment analysis. A novel π-like MO obtained by antisymmetric combination of C−H, C−Si σ-MOs (cf. similar destabilization of the HOMO of **5a**), and the Si−Si σ-MO contributes to the substantial destabilization of the HOMO of **7a** compared to that of **7b**.

***θ* = 60−120°, *ϕ* ca. 180°.** In both the calculated and X-ray conformations of **8a** (**9** and **10**, respectively), the θ values result in substantial C−Si σ-orbital interaction with the sulfur lone pair orbital. Furthermore, the ϕ values are the optimum for Si−Si σ-orbital interaction with the sulfur lone pair orbital mediated by the C−Si σ-orbital (recall the 0.6 eV decrease in ionization energy in the model compound comparing $\theta = 180°$, $\phi = 180°$ with $\theta = 90°$, $\phi = 180°$ noted above).

The calculated ionization energies for HOMO through HOMO-3 for each of the conformers **9** and **10** are 7.06, 7.23, 8.04, and 8.11 eV and 7.23, 7.33, 7.99, and 8.11 eV, respectively, while the orbital plots for conformation **9** are shown in Figure 6b (the results with **9** and **10** are very similar). The two highest energy MOs are very close in energy as are the next two MOs, and the separation of these averaged pairs is 0.93 and 0.77 eV for **9** and **10**, respectively. These separations are comparable to the experimental separation of 0.61 eV. The MOs for **9** shown in Figure 6b demonstrate that the HOMO and HOMO-1 are derived from all of the ring atoms and that the exocyclic Si−Si orbitals participate. Thus, the combined geminal Si−Si orbitals interact with the sulfur lone pair orbitals through the C−Si orbitals, accounting for the destabilization found in the calculations on model **1**, R = R′ = Me. The result of these extended interactions is that the HOMO ionization energy for **8a** is 0.39 eV lower than that for **8b**, which lacks the Si−Si orbitals but is calculated to have a ring geometry similar to that of **8a**.[23] In addition, the HOMO ionization for **8a** is 0.70 eV lower than that for 1,5-dithiocane **(8c)**.[16,31] This is the largest destabilization observed in this study, as expected from the predictions of theoretical calculations on model system **1**, R = R′ = Me. Fragment analyses for **8a** and **8b** are given in the Supporting Information.

Summary of Theoretical Studies. The theoretical calculations are able to predict the same ionization energy trends observed experimentally for the geometrically constrained mesocycles **2a**, **5**−**8a**, and **11a** having either exocyclic (**2a**, **8a**, **11a**) or endocyclic (**5**−**7a**) Si−Si bonds. Furthermore, these molecular orbital calculations provide insight into the complex geometry-dependent σ- and p-orbital interactions that are responsible for the experimentally observed ionization energies.

Conclusions

In summary, the experimental results demonstrate the presence of Si−Si σ-orbital destabilization of the sulfur 3p lone pair orbital when the Si−Si moiety is β to sulfur, and also that the amount of this destabilization is geometry dependent. Furthermore, the detailed theoretical studies presented on model compound **1**, R = R′ = Me, and the conformationally constrained compounds provide an understanding of the specific basis for destabilization, which involves mixing not only of Si−Si but other σ-orbitals, as well, as determined by energy, overlap, and symmetry. The chemical consequences of these interactions are under investigation.[39]

Experimental Section

Photoelectron Spectroscopy. PE spectra were recorded using an instrument that features a 36 cm hemispherical analyzer[46] and custom designed photon source, sample cells, and detection and control

(36) Sweigart, D. A.; Turner, D. W. *J. Am. Chem. Soc.* **1972**, *94*, 5599−5603.
(37) Gonbeau, D.; Loudet, M.; Pfister-Guillouzo, G. *Tetrahedron* **1980**, *36*, 381−391.
(38) Vondrak, T.; Bastl, Z. *J. Mol. Struct.* **1987**, *160*, 117−126.
(39) Owing to facile cleavage of the Si−C bond following anodic,[7f,h,40] chemical,[41] or photochemical[42] oxidation, synthetically useful methodology has been developed using oxidation of β-silyl ethers, thioethers, and amines. The Sn−C bond, in analogy with the Si−C bond, is easily cleaved on oxidation of stannylated ethers, amines, and sulfides electrochemically,[7h,43] chemically,[41,44] or photochemically, and this oxidative cleavage has also been exploited in synthesis.[45]
(40) (a) Yoshida, J.; Isoe, S. *Chem. Lett.* **1987**, 631−634. (b) Koizumi, T.; Fuchigami, T.; Nonaka, T. *Chem. Lett.* **1987**, 1095−1096. (c) Koizumi, T.; Fuchigami, T.; Nonaka, T. *Bull. Chem. Soc. Jpn.* **1989**, *62*, 219−225.
(41) (a) Narasaka, K.; Okauchi, T.; Arai, N. *Chem. Lett.* **1992**, 1229−1232. (b) Narasaka, K.; Arai, N.; Okauchi, T. *Bull. Chem. Soc. Jpn.* **1993**, *66*, 2995−3003.
(42) (a) Hasegawa, E.; Brumfeld, M. A.; Mariano, P. S. *J. Org. Chem.* **1988**, *53*, 5435−5442. (b) Yoon, U.-C.; Kim, H.-J.; Mariano, P. S. *Heterocycles* **1989**, *29*, 1041−1044. (c) Yoon, U.-C.; Kim, Y. C.; Choi, J. J.; Kim, D. U.; Mariano, P. S.; Cho, I.-S.; Jeon, Y. T. *J. Org. Chem.* **1992**, *57*, 1422−1428.
(43) (a) Yoshida, J.; Itoh, M.; Isoe, S. *J. Chem. Soc., Chem. Commun.* **1993**, 547−549. (b) Yoshida, J.; Itoh, M.; Morita, Y.; Isoe, S. *J. Chem. Soc., Chem. Commun.* **1994**, 549−551.
(44) Narasaka, K.; Kohno, Y.; Shimada, S. *Chem. Lett.* **1993**, 125−128.

electronics.[47] The excitation source is a quartz capillary discharge lamp with the ability, depending on operating conditions, to produce He I (21.218 eV) or He II (40.814 eV) photons. The ionization energy scale was calibrated using the $^2P_{3/2}$ ionization of argon (15.759 eV) and the $^2E_{1/2}$ ionization of methyl iodide (9.538 eV). The argon $^2P_{3/2}$ ionization also was used as an internal calibration lock of the absolute ionization energy to control spectrometer drift throughout data collection. During He I and He II data collection, the instrument resolution, measured using the full-width-at-half-maximum of the argon $^2P_{3/2}$ ionization, was 0.020−0.030 eV. All of the spectra were corrected for the presence of ionizations caused by other emission lines from the discharge source.[48] The He I spectra were corrected for the He Iβ line (1.866 eV higher in energy and 3% the intensity of the He Iα line), and the He II spectra were corrected for the He IIβ line (7.568 eV higher in energy and 12% the intensity of the He IIα line). All data also were intensity corrected with an experimentally determined instrument analyzer sensitivity function that assumes a linear dependence of analyzer transmission (intensity) to the kinetic energy of the electrons within the energy range of these experiments. The samples all sublimed cleanly with no visible changes in the spectra during data collection.

In the figures of the data, the vertical length of each data mark represents the experimental variance of that point.[49] The valence ionization bands are represented analytically with the best fit of asymmetric Gaussian peaks, as described in more detail elsewhere.[49] The Gaussians are defined with the position, amplitude, half-width for the high binding energy side of the peak, and the half-width for the low binding energy side of the peak. The peak positions and half-widths are reproducible to about ±0.02 eV ($\approx 3\sigma$ level). The parameters describing an individual Gaussian are less certain when two or more peaks are close in energy and are overlapping. When a region of broad ionization intensity spans numerous overlapping ionization bands, the individual parameters of the Gaussian peaks used to model the total ionization intensity are not characteristic of individual ionization states. Confidence limits for the relative integrated peak areas are about 5%, with the primary source of uncertainty being the determination of the baseline under the peaks. The baseline is caused by electron scattering and taken to be linear over the small energy range of these spectra. The total area under a series of overlapping peaks is known with the same confidence, but the individual peak areas are less certain.

Computational Methodology. Calculations were performed with Gaussian 03 (revision B.04).[50] All computations were carried out using Becke's three-parameter hybrid method with Perdew and Wang's exchange-correlation functional (B3PW91).[51] All computations were carried out using the CEP-121G split-valence basis set with effective core potentials.[52] Vertical ionization potentials were computed by the ΔSCF method (total difference between the cation radical energy at the neutral minimized geometry and the neutral energy at that geometry), but orbital energies were estimated from the orbital eigenvalues (by a modification of Koopman's theorem; see below); the vertical IPs are therefore expected to be more reliable than the orbital energies. The method which was used to estimate most of the orbital energies takes the difference between the HOMO eigenvalue and the orbital eigenvalue and adds this to the computed molecular vertical IP (essentially constituting an offset correction to the normal Koopman's theorem values). Orbitals were visualized using MOLEKEL 4.3.win32.[53] Fragment analysis of the wave function was accomplished using the method of Senthilkumar and Bickelhaupt[54] to express the Gaussian output in the Kohn−Sham matrix form of the type $H_{KS}C = SCE$, where H_{KS} is the Kohn−Sham Hamiltonian matrix, C is the eigenvector matrix, S is the overlap matrix, and E is the diagonal eigenvalue matrix. The matrices were transformed to the basis of the sulfur or selenium atoms and the silicon-substituted alkyl fragments using the calculated equilibrium coordinates for the entire molecule. This method has been used previously for fragment analyses of other chemical systems.[55]

Acknowledgment. The authors gratefully acknowledge support of this work by the donors of the Petroleum Research Fund administered by the American Chemical Society (R.S.G., E.B.), the National Science Foundation (CHE-0201555, CHE-0455575, R.S.G.; CHE-9906566, CHE-0342660, CHE-0450505, E.B.), and NCSA, through a supercomputing grant (E.L.). This work was done, in part, at the Center for Gas-Phase Electron Spectroscopy, The University of Arizona.

Supporting Information Available: PES and table of fitting parameters for **6a**; figures containing plots of the sulfur- or selenium-free fragment orbitals that contribute to molecular orbitals of **2a**−**d**, **5a**, **7a**, **8a**, and **8b**, their percent contributions, and contribution to the molecular orbital eigenvalues; molecular orbital plots of the HOMO, HOMO-1, and HOMO-2 of **2b**; table of calculated geometric parameters for **5a** compared with those determined by X-ray crystallography; table of experimental and calculated ionization energies for **2a**,**b**, **5a**, **7a**, and **8a**; full author list for ref 50. This material is available free of charge via the Internet at http://pubs.acs.org.

JA0573514

(45) Ikeno, T.; Harada, M.; Arai, N.; Narasaka, K. *Chem. Lett*. **1997**, 169−170.
(46) Siegbahn, K.; Nordling, C.; Fahlman, A.; Nordberg, R.; Hamrin, K. *ESCA: Atomic, Molecular and Solid State Structure Studied by Means of Electron Spectroscopy*; Almqvist & Wiksells: Uppsala, Sweden, 1967.
(47) Lichtenberger, D. L.; Kellogg, G. E.; Kristofzski, J. G.; Page, D.; Turner, S.; Klinger, G.; Lorenzen. J. *Rev. Sci. Instrum.* **1986**, *57*, 2366.
(48) Turner, D. W.; Baker, C.; Baker, A. D.; Brundle, C. R. *Molecular Photoelectron Spectroscopy*; Wiley-Interscience: London, 1970.
(49) Lichtenberger, D. L.; Copenhaver, A. S. *J. Electron Spectrosc. Relat. Phenom.* **1990**, *50*, 335−352.
(50) Frisch, M. J.; et al. *Gaussian 03*, revision B.04; Gaussian, Inc.: Pittsburgh, PA, 2003.
(51) Becke, A. D. *J. Chem. Phys.* **1993**, *98*, 5648−5652.
(52) Confirmation that this computational method adequately describes the compounds reported in this paper is found in the Supporting Information. This information consists of two parts; first, the calculated geometry and that determined by X-ray crystallography[23] for **5a** are comparable, and second, the experimentally determined and computed ionization energies for **2a**,**b**, **5a**, **7a**, and **8a** are correlated.
(53) (a) Flükiger, P.; Lüthi, H. P.; Portmann, S.; Weber, J.; *MOLEKEL 4.3*; Swiss Center for Scientific Computing: Manno, Switzerland, 2000−2002. (b) Portmann, S.; Lüthi, H. P. *Chimia* **2000**, *54*, 766−769.
(54) Senthilkumar, K.; Grozema, F. C.; Bickelhaupt, F. M.; Siebbeles, L. D. A. *J. Chem. Phys.* **2003**, *119*, 9809−9817.
(55) (a) Janczyk, A.; Lichtenberger, D. L.; Ziurys, L. M. *J. Am. Chem. Soc.* **2006**, *128*, 1109−1118. (b) Cotton, F. A.; Donahue, J. P.; Gruhn, N. E.; Lichtenberger, D. L.; Murillo, C. A.; Timmons, D. J.; Van Dorn, L. O.; Wang, X. P. *Inorg. Chem.* **2006**, *45*, 201−213. (c) Rajapakshe, A.; Paz-Sandoval, M. A.; Gutierrez, J. A.; Navarro-Clemente, J. E.; Saavedra, P. A.; Gruhn, N. E.; Lichtenberger, D. L. *Organometallics* **2006**, *25*, 1914−1923.